https://doi.org/10.20965/jrm.2016.p0351

Paper:

Effectiveness of Delayed Feedback Control Applied to a Small-Size Helicopter with a Suspended Load System

Motomichi Sonobe*, **Masafumi Miwa****, **and Junichi Hino****

*Kochi University of Technology
Tosayamada-cho, Kami-shi, Kochi 782-8502, Japan
E-mail: sonobe.motomichi@kochi-tech.ac.jp
**Tokushima University
2-1 Minami-Josanjima-cho, Tokushima-shi, Tokushima 770-8506, Japan
[Received August 28, 2015; accepted March 18, 2016]

In this study, a cable-suspended transportation system using a small-size helicopter was investigated. For a secure flight, it is necessary to suppress the swing of the suspended load. For this purpose, a cable angle feedback system was adopted because it is easy to mount the corresponding measuring device on a helicopter. Delayed feedback control was applied for efficient swing damping. The control parameters were obtained using a simple planar double pendulum model that takes into consideration the coupled dynamics of the helicopter and the load. To build the model, the system parameters were identified through frequency response flight tests. In this paper, an appropriate design strategy is reported for a trade-off relationship between vibration damping and piloted handling qualities; the robustness of the control method against disturbances and signal noise was verified by comparing the delayed feedback control method with the real-time angular velocity feedback control method. The damping effect was verified by performing flight tests with three cable lengths.

Keywords: small-size helicopter, delayed feedback control, swing damping, double pendulum

1. Introduction

This paper presents the development of a secure transportation system using a small-size helicopter with a suspended load. Such a flight transportation system is expected to have practical applications for conveyance in islands or mountainous regions, but its load should be light to ensure a secure flight [1, 2], because swing damping control is generally not considered in the design of the system. Therefore, developing a method of suppressing the swing of the suspended load would allow such systems to be used to transport heavier loads.

Most previous studies on heavy-lift helicopters were published in the 1960s and 1970s. In an early work, Dukes demonstrated stability analysis during hovering and low-speed flights [3, 4]. Poll and Cromack analyzed helicopter stability in high-speed flights [5], and Cicolani et al. reported the influence of air flow dynamics acting on the suspended load [6]. Regarding swing damping, Ivler et al. investigated the optimum parameters of the cable angle/rate feedback for vibration damping. They indicated that there is a trade-off relationship between vibration damping and piloted handling qualities [7, 8].

In recent years, several studies have been conducted on transportation systems using small-size helicopters. Bernard et al. proposed a cable tension control to carry a heavy load using multiple small-size helicopters [9]. Bisgaard et al. [10] built a three-dimensional model of a small-size helicopter and a suspended load system using the Udwadia-Kalaba method [11], which allows the constraint force via cable to be expressed explicitly. In addition, they proposed an adaptive control system that can adapt to changes in the mass of the load by measuring the cable tension. They also applied an input shaping method and delayed feedback control for swing damping [12]. Applying input shaping to the suspended flight system was reported in another study [13].

Delayed feedback control is applied for chaos control, which leads to steady motion. However, Udwadia et al. reported that a small delay has a damping effect on a simple vibration system using the delayed feedback control for displacement or velocity [14, 15]. Additionally, Ulsoy reported that the combination of real-time feedback control and delayed feedback control allows improvement in stability margins of a control system [16]. The point is useful in the development of a swing damping system for a transportation system using a small-size helicopter, because the feedback gain for swing damping is small. Therefore, it can be assumed that the approach employed by Bisgaard et al. to swing damping is theoretically appropriate [12]. However, the swing of the load had no effect on the dynamics of the helicopter in their model. Thus, the performance of the delayed feedback control cannot be adequately evaluated if the load is relatively heavy. Additionally, although they designed the control parameters using the eigenvalue of the system, the trade-off relationship between swing damping and position control was not considered.

The purpose of this study is to clarify the delayed feed-

Fig. 1. T-Rex600CF helicopter.

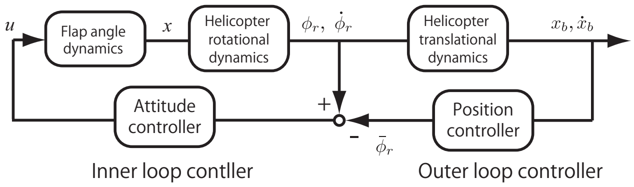

Fig. 2. Block diagram of the flight control system.

back control design process for swing damping in a small-size helicopter. To take the coupled dynamics and the abovementioned trade-off relationship into consideration in the proposed design process, a simple double pendulum model was built. The parameters were identified through a frequency response test. Although the control and design methods were described in a previous paper [17], the design method was not sufficient, as the piloted handling qualities were not discussed. In addition, the advantages of the delayed feedback control method were not clear.

In this study, a delayed feedback controller was designed based on the damping ratio to ensure adequate piloted handling qualities. Because the delayed feedback control system tends to be sensitive to disturbances, its robustness against disturbances and signal noise was investigated. Finally, the effectiveness of the present method was verified by performing a flight test with three cable lengths.

The framework of this paper is as follows. In Section 2, the modeling of the helicopter's single flight control system and the parameter identification process are presented. Section 3 describes the swing damping control strategy, including the control method, the controller design process, and an evaluation of the robustness of the delayed feedback controller. The experimental results are presented in Section 4.

2. Helicopter Modeling and Identification

2.1. Flight Control System

The Align T-Rex600CF helicopter shown in **Fig. 1** was used in this experiment. A microcomputer, a heading reference system (Microstrain 3DM-GX3-25), a global positioning system (GPS) unit (Garmin GPS18x-5Hz), and a pressure sensor (VTI Technologies SCP1000) were mounted on the helicopter. The cycle time of the control system was set to 50 ms, except for the GPS data, for which it was set to 200 ms. The classical control theory based on proportional and derivative feedback control, which is the most popular control technique in flight control of small-size helicopters, was applied to the system. The roll, pitch, yaw, and vertical dynamics of the controller were independently designed. The position of the helicopter was controlled as an outer loop via the reference angle of the attitude control [18]. In the discussion below on the swing damping control in a suspended load system, the roll and pitch control system is considered. A block diagram of the roll and pitch dynamics of the flight control is shown in **Fig. 2**.

As the feedback parameters were experimentally determined by trial and error, the system parameters were unknown. The center of gravity and moment of inertia were derived using free vibration tests, and the other system parameters were identified through the frequency response test. The models were built with reference to a past study [19]. As the expressions for roll (lateral) and pitch (longitudinal) dynamics are equivalent in the model, roll dynamics was considered for simplicity. The translational, rotational, and flapping dynamics of the main rotor for the roll dynamics are described by

$$\ddot{x}_b = Mg\phi_r \quad \ldots\ldots\ldots\ldots\ldots \quad (1)$$

$$J_r\ddot{\phi}_r = G_a a \quad \ldots\ldots\ldots\ldots\ldots \quad (2)$$

$$T_a\dot{a} = -a - T_a\dot{\phi}_r + \alpha u_r(t-\tau_{lr}), \quad \ldots\ldots \quad (3)$$

where x_b is the position of the helicopter (expressed in body-fixed coordinates), ϕ_r is the roll angle of the helicopter, a is the flap angle of the main rotor, u_r is the cyclic pitch input, and g is the gravitational acceleration. The constant parameters in Eqs. (1), (2) and (3) are as follows: M is the mass of the helicopter, J_r is the moment of inertia about the center of gravity, τ_{lr} is the dead time of the flap angle control, T_a is the time constant of the flap angle dynamics, and G_a and α are physical constants. The mass and the moment of inertia were measured by free vibration tests, and the following values were obtained: $M = 6.06$ kg, $J_r = 0.11$ kgm^2, and $J_p = 0.61$ kgm^2.

The input u_r includes the attitude (inner loop) and position (outer loop) control, as given below.

$$u_r = -k_{dr}\dot{\phi}_r - k_{pr}(\phi_r - \bar{\phi}_r) \qquad \text{(inner loop)} \quad . \quad (4)$$

$$\bar{\phi}_r = -K_{dx}\dot{x} - K_{px}\{x_b - \bar{x}_b\} \qquad \text{(outer loop)}, \quad . \quad (5)$$

where k_{dr}, k_{pr}, K_{dx}, and K_{px} are feedback parameters and $\bar{\phi}_r$ and $\bar{x}_b$ are the reference angle and reference position, respectively. The values of the feedback control parameters were obtained as follows: $k_{dr} = k_{dp} = 17.0$, $k_{pr} = k_{pp} = 1031$, $K_{dr} = K_{dp} = 0.0105$, and $K_{pr} = K_{pp} = 0.785$. From Eqs. (1), (2) and (3), the transfer function from u_r to ϕ_r is given by

$$G_r(s) = \frac{b_1 e^{-b_2 s}}{s^3 + a_2 s^2 + a_1 s}. \quad \ldots\ldots\ldots \quad (6)$$

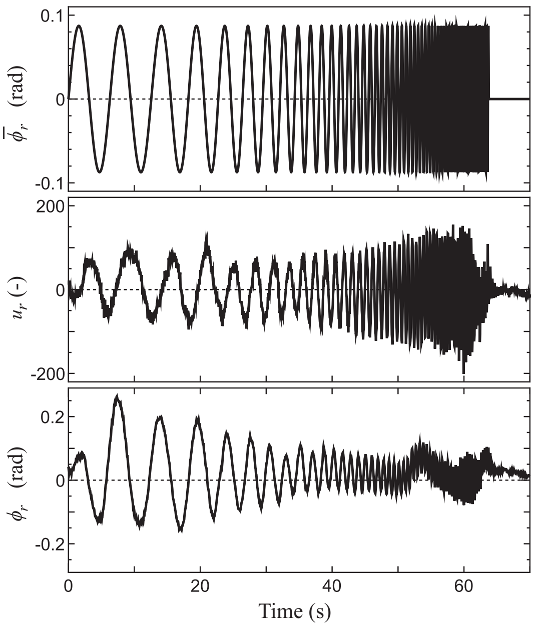

Fig. 3. Reference angle, input, and helicopter angle during frequency response test (roll).

The unknown parameters (T_a, G_a, α, and τ_{lr}) were estimated by fitting Eq. (6) to the frequency response function obtained from the frequency response test described in Section 2.2.

2.2. Frequency Response Test

In the frequency response test, a frequency sweep input of 1.0 to 25 rad/s was applied to the reference angle $\bar{\phi}_r$. The frequency sweep input [20] is defined as follows:

$$\begin{cases} \bar{\phi} = A \sin \psi \\ \psi = \int_0^{T_{rec}} \omega \, dt \\ \omega = \omega_{\min} + K(\omega_{\max} - \omega_{\min}) \\ K = 0.0187 \left\{ \exp\left(\dfrac{4t}{T_{rec}}\right) - 1 \right\}, \end{cases} \quad \ldots\ldots (7)$$

where T_{rec} is the period of the Fourier analysis. We set $\omega_{\max} = 25.0$ rad/s, $\omega_{\min} = 1.0$ rad/s, $T_{rec} = 51.2$ s, and $A = 5°$ during the test. Before starting the frequency sweep, two periods of a sine wave ($\bar{\phi} = A \sin \omega_{\min} t$) with a constant frequency $\omega_{\min}$ were given to obtain the response data accurately. The flight tests were independently implemented for roll and pitch dynamics.

The reference angle $\bar{\phi}_r$, input u_r, and the attitude angle of the helicopter ϕ_r during the test are shown in **Fig. 3**. Frequency response functions (FRFs) were derived from the time series data of the input u_r and the output ϕ_r. Additionally, the tests were validated by evaluating the coherence, which is defined as

$$Coh = \frac{|G_{U\Phi}|^2}{G_{UU} \cdot G_{\Phi\Phi}}, \quad \ldots\ldots (8)$$

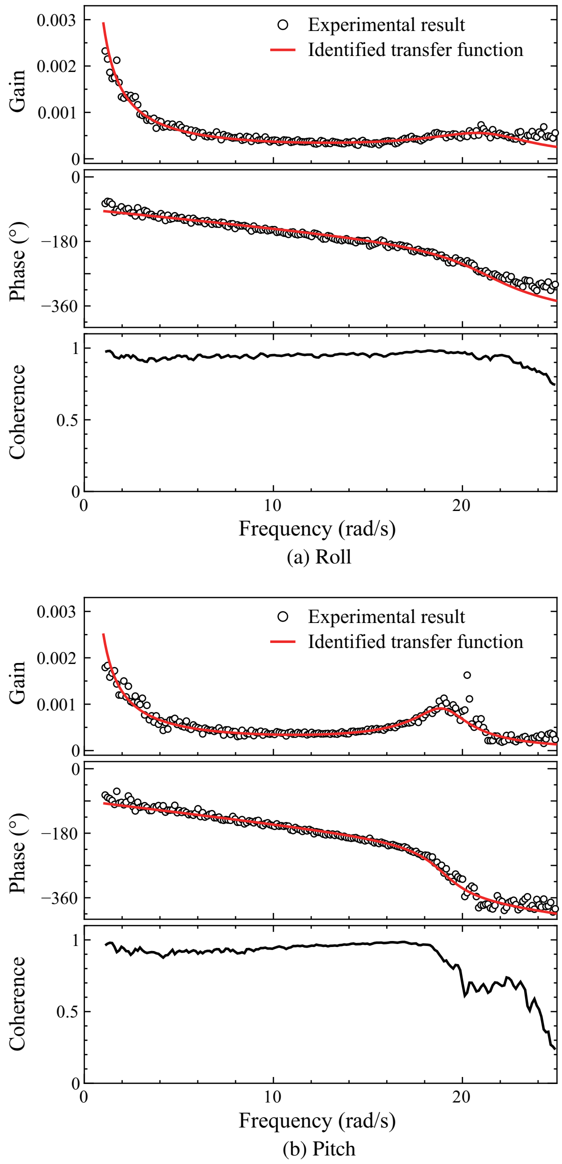

Fig. 4. FRFs and coherence obtained from the frequency response test.

where $G_{U\Phi}$ is the cross spectrum between u and ϕ, and G_{UU} and $G_{\Phi\Phi}$ are the power spectra of u and ϕ, respectively. When the coherence exceeds 0.6, the input and output are considered to be correlated. **Fig. 4** shows the FRF and the coherence obtained from the tests performed in this study. The experimental results are plotted as circles, and the fitted functions are represented by solid lines. The fitted function as per Eq. (6) was calculated using the Levenberg-Marquardt method. The coherence exceeds 0.6 for frequencies between 1 and 23 rad/s, which indicates that the experimental data are valid. Consequently, the transfer functions for the roll and pitch dynamics were obtained as follows.

$$\frac{\Phi_r}{U_r} = \frac{1.36e^{-0.0808s}}{s^3 + 5.45s^2 + 461.5s} \quad \ldots\ldots (9)$$

$$\frac{\Phi_p}{U_p} = \frac{0.914e^{-0.104s}}{s^3 + 2.78s^2 + 362s}. \quad \ldots\ldots (10)$$

Table 1. Identified system parameters.

τ_{lr}	0.081	T_a	0.184	G_a	461	α	0.00539
τ_{lp}	0.102	T_b	0.376	G_b	357	β	0.00927

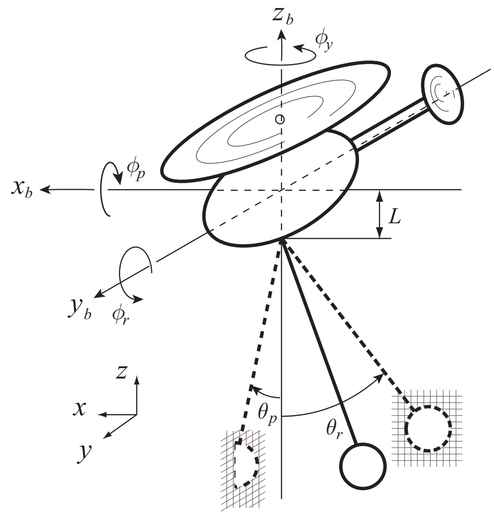

Fig. 5. Coordinate definition for helicopter and suspended load system.

From these functions, the system parameters shown in **Table 1** were obtained. The parameters τ_{lp}, T_b, G_b, and β in the table represent the pitch dynamics.

3. Swing Damping for Suspended Load System

3.1. Swing Damping Control

This section describes the load suspended by a cable that is mounted on the helicopter. Since it is difficult to mount the cable exactly at the center of gravity of the helicopter, the pivot of the cable was connected to the helicopter directly below the center of gravity. The vertical clearance between the center of gravity and the pivot is $L = 0.157$ m. **Fig. 5** shows a schematic of this system. The coordinates are defined such that (x, y, z) are the global coordinates, and (x_b, y_b, z_b) are the rotational coordinates that depend on the attitude of the helicopter.

Angles θ_r and θ_p are the rotational angles about the y_b- and x_b-axes, respectively. The origin of the cable angles is fixed in the vertical direction.

For swing damping, delayed feedback control for cable angle was added to the system as an outer loop. The cable angles were measured by a swinging device with two potentiometers, as shown in **Fig. 6**. Although the angular velocity feedback is more effective than the angle feedback, cable angle feedback was adopted because of the simplicity of the measurement system regarding the mounting position of the device and the coordinate conversion from global to rotational coordinates.

To add swing damping control, the control system de-

Fig. 6. Cable angle measuring device.

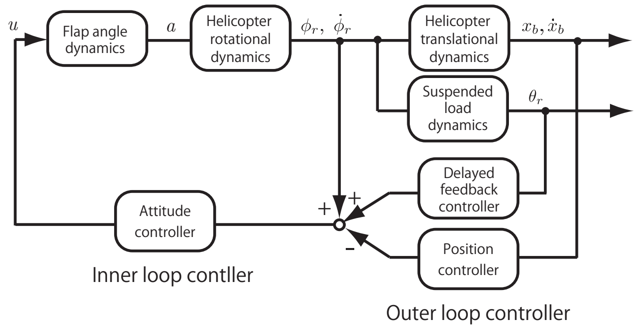

Fig. 7. Block diagram of helicopter and suspended load system.

scribed in Eqs. (3) and (4) was modified as follows:

$$u_r = -k_{dr}\dot{\phi}_r - k_{pr}(\phi_r - \bar{\phi}_r) \quad \dots\dots\dots \quad (11)$$

$$\bar{\phi}_r = -K_{dx}\dot{x}_b(t) - K_{px}\{x_b(t) - \bar{x}_b\} + G_{dr}\theta_r(t - \tau_{dr}) . \quad \dots\dots\dots \quad (12)$$

The third term on the right-hand side of the second equation contributes to the attenuation of the cable swing. A block diagram of this swing control system is shown in **Fig. 7**. The control parameters for swing damping are composed of a feedback gain G_{dr} and a delay time τ_{dr}. The design strategy for these parameters is discussed below.

3.2. Swing Damping Model

The delayed feedback control parameters should be designed theoretically, because adjusting the parameters during a flight test with a suspended load involves risks. Bisgaard et al. determined the parameters to minimize the real part of all the eigenvalues in the system [9]. Since they ignored the interaction between the helicopter and the suspended load, the effectiveness of their design was restricted to situations in which the weight of the load is relatively less. However, swing damping is less important in such situations.

The control parameters were designed considering the interaction between the helicopter and the load. To achieve it, the dynamics was divided into roll and pitch

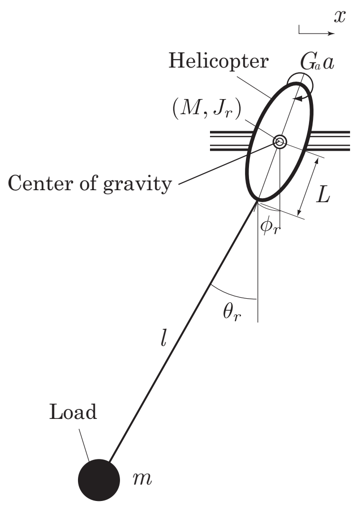

Fig. 8. Double pendulum model for delayed feedback controller design (roll).

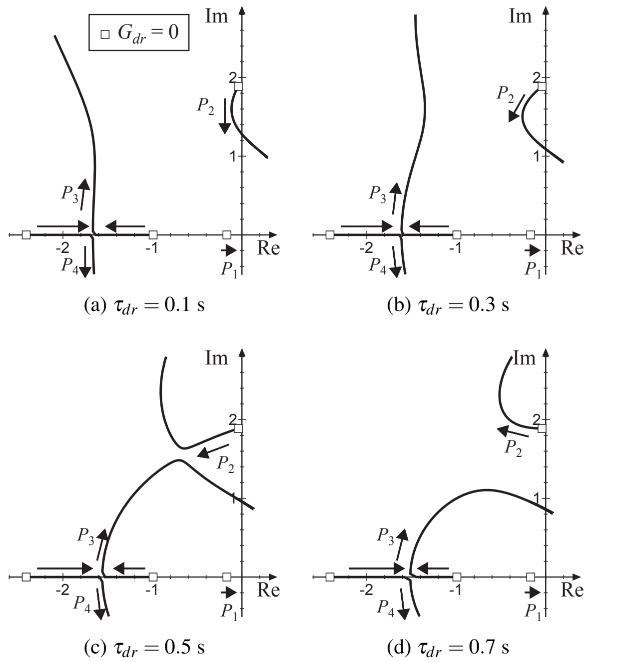

Fig. 9. Root loci of the delayed feedback system (roll).

dynamics, and a planar model was built. The model shown in **Fig. 8** makes it possible to consider the interaction between the helicopter and the load. The mass of suspended load is $m = 0.74$ kg, and the distance between the center of gravity of the helicopter and the pivot of the cable is $L = 0.157$ m in the model. The model is a three-degree-of-freedom system composed of horizontal translational dynamics, rotational dynamics, and the swinging of a pendulum. The vertical translational dynamics of the helicopter was neglected in the model, because it has little effect on the swinging of the load. Taking the frapping dynamics into consideration, the equations of motion in the model are given by

$$(M+m)\ddot{x} - mL\ddot{\phi}_r - ml\ddot{\theta}_r = (M+m)g\phi_r \quad \ldots \quad (13)$$

$$-mL\ddot{x} + (J_r + mL^2)\ddot{\phi}_r + mLl\ddot{\theta} + mgL\phi_r = J_r G_a a \quad (14)$$

$$-ml\ddot{x} + mLl\ddot{\phi}_r + ml^2\ddot{\theta}_r + mgl\theta_r = 0 \quad \ldots \quad (15)$$

$$T_a\dot{a} = -a - T_a\dot{\phi}_r + \alpha u_r(t - \tau_{lr}). \quad \ldots \quad (16)$$

The cable length l and the mass m of the load were set to 3.0 m and 0.74 kg, respectively. Substituting Eqs. (11) and (12) into Eq. (16) and representing the resulting equation in the Laplace domain, the following is obtained:

$$\begin{bmatrix} q_{r11} & q_{r12} & q_{r13} \\ q_{r21} & q_{r22} & q_{r23} \\ q_{r31} & q_{r32} & q_{r33} \end{bmatrix} \begin{bmatrix} X \\ \Phi \\ \Theta \end{bmatrix} = \begin{bmatrix} 0 \\ 0 \\ 0 \end{bmatrix}, \quad \ldots \quad (17)$$

where

$$\begin{aligned}
q_{r11} &= (M+m)s^2 \\
q_{r12} &= -mLs^2 - (M+m)g \\
q_{r13} &= -mls^2 \\
q_{r21} &= -(T_a s + 1)mLs^2 \\
&\quad + J_r G_a \alpha k_{pr}(K_{dx}s + K_{px})e^{-\tau_{lr}s} \\
q_{r22} &= (T_a s + 1)\left\{\left(J_r + mL^2\right)s^2 + mgL\right\} \\
&\quad + J_r G_a\left\{T_a s + \alpha(k_{dr}s + k_{pr})e^{-\tau_{lr}s}\right\} \\
q_{r23} &= (T_a s + 1)mLls^2 - J_r G_a \alpha k_{pr} G_{dr} e^{-(\tau_{lr}+\tau_{dr})s} \\
q_{r31} &= -mls^2 \\
q_{r32} &= mLls^2 \\
q_{r33} &= ml^2 s^2 + mgl.
\end{aligned}$$

The characteristic equation of Eq. (17) is given by

$$\begin{vmatrix} q_{r11} & q_{r12} & q_{r13} \\ q_{r21} & q_{r22} & q_{r23} \\ q_{r31} & q_{r32} & q_{r33} \end{vmatrix} = 0. \quad \ldots \quad (18)$$

To solve Eq. (18), the exponential functions $e^{-\tau_{lr}s}$ and $e^{-(\tau_{lr}+\tau_{dr})}$ arising from the time delay are transformed into a polynomial by the third-order Padé approximation as follows:

$$e^{-\tau s} = \frac{1 - \frac{1}{2}\tau s + \frac{1}{10}(\tau s)^2 - \frac{1}{120}(\tau s)^3}{1 + \frac{1}{2}\tau s + \frac{1}{10}(\tau s)^2 + \frac{1}{120}(\tau s)^3}. \quad \ldots \quad (19)$$

Thus, 13 characteristic roots of the system were obtained.

3.3. Delayed Feedback Controller Design

A delayed feedback controller for desirable dynamics is discussed in this section. A key issue is how to attenuate the cable swing while ensuring acceptable piloted handling qualities. To discuss this issue, the relationship between the delayed feedback parameters and the system dynamics is clarified by drawing the root loci of the system.

Figure 9 shows the root loci as G_{dr} is increased from 0 to 1.0 with fixed delay times τ_{dr} of 0.1, 0.3, 0.5, and 0.9 s. Each part of the figure shows the loci of four roots (named P_1, P_2, P_3, and P_4), which are significant, because the real parts of the four roots are larger than those of the other nine roots. The four roots represent the vibra-

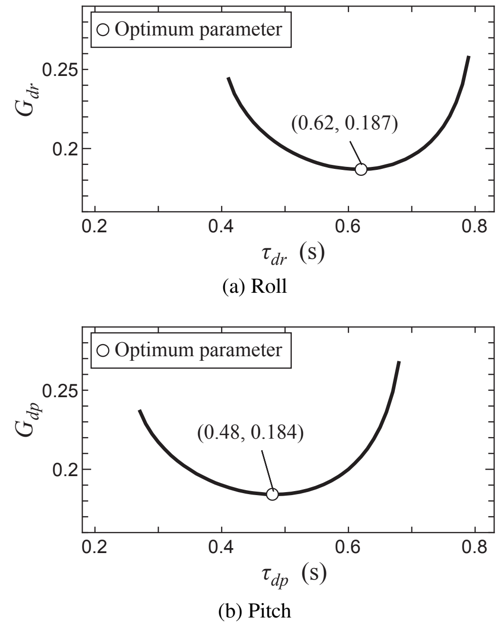

Fig. 10. Delayed feedback gains by setting the damping ratio to 0.2 ($l = 3.0$ m).

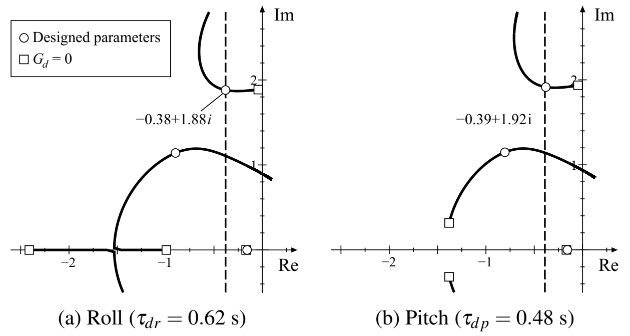

Fig. 11. Root loci of the delayed feedback system (roll).

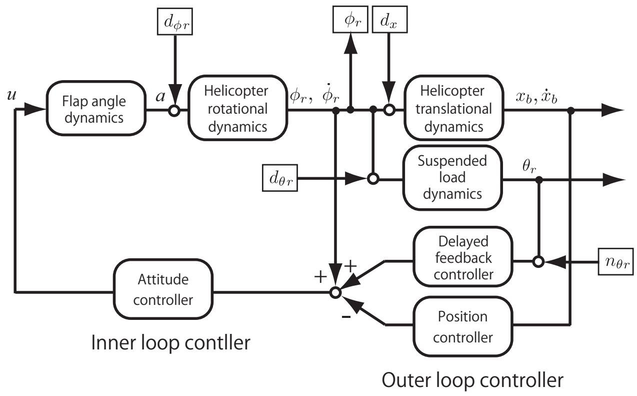

Fig. 12. Block diagram of the controller considering disturbances and signal noise.

tion damping effect and the helicopter's maneuverability. The squares in the figures are roots where $G_{dr} = 0$. P_1, P_3, and P_4 indicate the position control dynamics, and P_2 indicates the first-order vibration mode of the double pendulum system.

Regardless of the control parameters, real root P_1 remains almost constant around -0.2. Conversely, P_2, P_3, and P_4 vary according to the parameters. When the delay time is set to 0.5 or 0.7 s, P_2 moves left, and P_3 and P_4 move right after their paths intersect with increasing G_{dr}. This indicates that adding the vibration damping effects deteriorates the maneuverability of the position control.

Considering that there is no need for a high damping effect in swing damping, the damping effect required for a secure flight should be obtained with as small a feedback gain as possible. It was assumed that the required damping ratio of the swing was approximately 0.2, based on the natural frequency with $G_{dr} = G_{dp} = 0$. The delayed feedback controller was designed to achieve the damping ratio by setting G_{dr} and G_{dp} as small as possible. For reference, P_2 without swing damping control is $-0.0413 + 1.89i$ (roll) or $-0.0474 + 1.94i$ (pitch) when the cable length is 3.0 m. To set the damping ratio to 0.2, the real parts of P_2 were designed to -0.38 (roll) and -0.39 (pitch), respectively.

Figure 10 shows the delayed feedback parameters required to yield a system damping ratio of 0.2. To minimize G_{dr}, the delay times were set to 0.62 and 0.48 s for roll and pitch dynamics, respectively. The gains were set as $G_{dr} = 0.187$ and $G_{dp} = 0.184$. The root loci for fixed delay times of $\tau_{dr} = 0.62$ s and $\tau_{dp} = 0.48$ s are shown in **Fig. 11**. The characteristic roots at the design parameters are plotted as circles. The results indicate that the real part of P_4 increases to -0.8 when the damping ratio of the cable swing is set to 0.2.

3.4. Robustness Against Disturbance and Noise

Delayed feedback control tends to be sensitive to disturbance and signal noise. The robustness of the delayed feedback control was evaluated against disturbances and signal noise using a double pendulum model. As the results for the roll and pitch dynamics were similar, only the roll dynamics is discussed in this section.

A block diagram of the system including disturbances and signal noise is shown in **Fig. 12**. It was assumed that three external forces d_x, d_ϕ, and d_θ act on helicopter, affecting its translational dynamics, its rotational dynamics, and the swing of its load, respectively. Furthermore, it was assumed that a noise signal $n_{\theta r}$ is mixed with the cable angle signal. The sensitivity of the attitude angle ϕ was evaluated against the three disturbances and the noise. For comparison, real-time velocity feedback control was applied instead of the control defined in Eqs. (11) and (12). This velocity feedback control is given by

$$u_r = -k_{dr}\dot{\phi}_r - k_{pr}(\phi_r - \bar{\phi}_r) \quad \ldots \ldots \ldots \quad (20)$$

$$\bar{\phi}_r = -K_{dx}\dot{x} - K_{px}(x - \bar{x}) + G_{vr}\dot{\theta}_r . \quad \ldots \ldots \quad (21)$$

To set the damping ratio to 0.2, G_{vr} was set as -0.127.

The sensitivity of the attitude angle of the helicopter to an external force, given by a sinusoidal wave, for the two different control methods is shown in **Fig. 13**. From the results, the delayed feedback control was found to be more sensitive than the real-time feedback control in the low frequency range (below the natural frequency $\omega_n \approx 1.9$ rad/s); however, the results showed the opposite

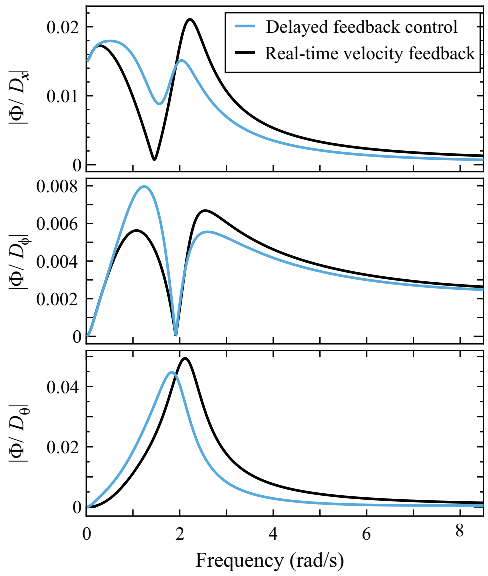

Fig. 13. Disturbance sensitivity of the attitude angle of the helicopter for different control methods.

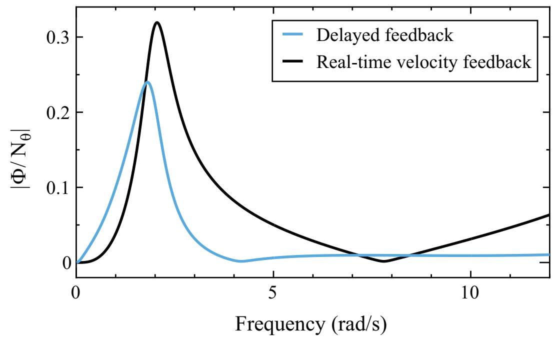

Fig. 14. Noise sensitivity of the attitude angle generated by the cable angle.

tendency in the high frequency range. **Fig. 14** shows the sensitivity of the control method to signal noise. These results also indicate that the delayed feedback control is superior to the real-time feedback control in the high frequency range.

It can be considered that the sensitivities of the two feedback control methods to the external force do not differ significantly, but the difference between their sensitivities to noise is relatively large. As a result, it was found that the robustness of the delayed feedback control against external forces is comparable to that of the real-time feedback control, and that the delayed feedback control is superior to the real-time feedback control in terms of robustness against signal noise.

4. Flight Test

To verify the effectiveness of the present control method, a cable-suspended flight test was performed. Swing damping control started after the load was pushed to intentionally start its swinging. The cable lengths were

Table 2. Parameters of the delayed feedback controller.

Cable length	Roll / Lateral		Pitch / Longitudinal	
	G_{dr}	τ_{dr} (s)	G_{dp}	τ_{dp} (s)
2.0 m	0.207	0.40	0.219	0.25
3.0 m	0.187	0.60	0.184	0.50
4.6 m	0.168	0.95	0.152	0.85

fixed at 2.0, 3.0, and 4.6 m, and the delayed feedback controller was designed in advance according to the cable length. The control design parameters are listed in **Table 2**. As the cycle time was 50 ms in the test, the delay time was rounded to the nearest multiple of 50 ms. The test flights were repeated five times in each condition.

Representative examples of the experimental results for cable lengths of 2.0, 3.0, and 4.6 m are shown in **Figs. 15**, **16**, and **17**, respectively. In all the experiments, the swing damping control began at $t = 5.0$ s. Under the damping control, the swing of the load was attenuated during hovering. The results indicate that our design strategy for delayed feedback control has a good effect regardless of the difference in cable length.

5. Conclusion

In this study, a suspension load transfer system using a small-size helicopter was investigated. To attenuate the swing of the load, delayed feedback control of cable angle was adopted, owing to the simplicity of its measuring system. Although the influence of the swing of the load on the helicopter dynamics has generally been ignored in the past studies, this influence was considered in the present study by applying a double pendulum model. This made it possible to design the delayed feedback controller for a relatively heavy load. To accurately build the model, the system parameters of the helicopter were identified through a frequency response test without a load.

In the design strategy for the delayed feedback control, the trade-off relationship between position control and swing damping of the load was considered. A damping ratio of 0.2 was assumed and the delayed feedback controller was designed to achieve the damping effect with minimum feedback gain. Regarding sensitivity to disturbances and signal noise, the delayed angle feedback control was shown to be superior to the real-time velocity feedback control when the double pendulum model is adopted. Additionally, the effectiveness of our control and design method was verified by conducting a flight test.

In this paper, a swing damping control method and a design approach for a cable-suspended transportation system using a small-size helicopter were presented. Although it is easy to apply the control method to the system, the design approach requires identification of the helicopter parameters through flight tests. This technique is expected to be useful in practical applications.

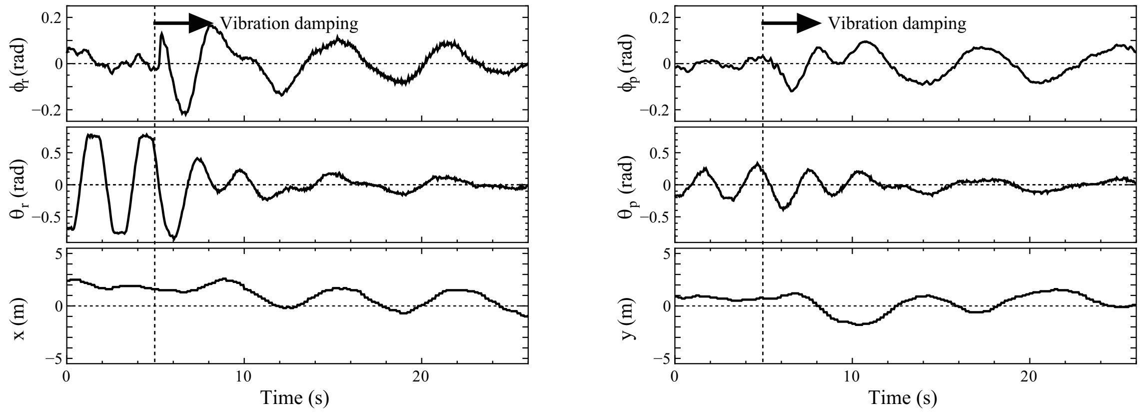

(a) Roll/Lateral (b) Pitch/Longitudinal

Fig. 15. Experimental results of the flight test with a suspended load ($l = 2.0$ m).

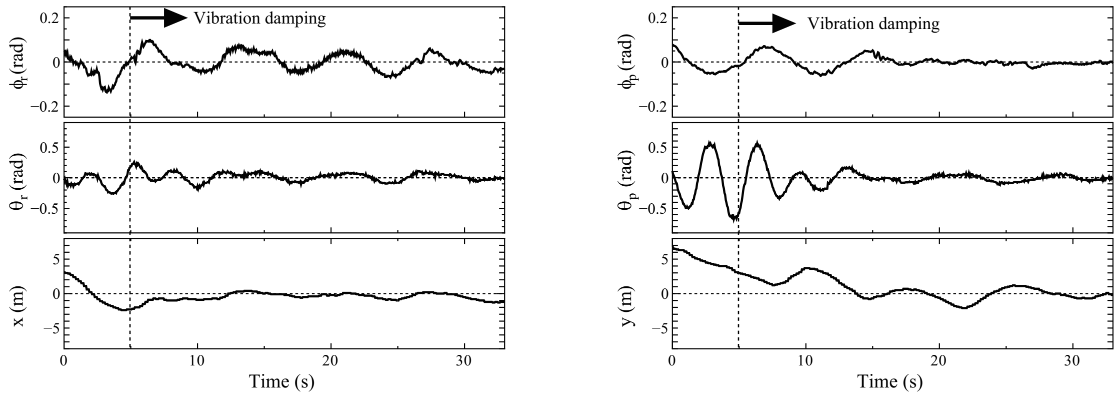

(a) Roll/Lateral (b) Pitch/Longitudinal

Fig. 16. Experimental results of the flight test with a suspended load ($l = 3.0$ m).

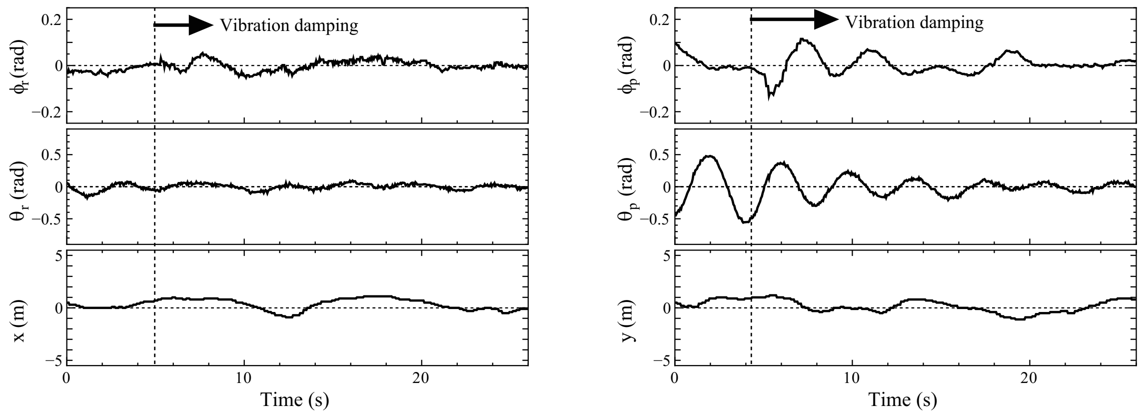

(a) Roll/Lateral (b) Pitch/Longitudinal

Fig. 17. Experimental results of the flight test with a suspended load ($l = 4.6$ m).

References:

[1] K. Nonami, "Prospect and Recent Research & Development for Civil Use Autonomous Unmanned Aircraft as UAV and MAV," J. of System Design and Dynamics, Vol.1, No.2, 2007.

[2] D. Fujiwara, J. Shin, K. Hazawa, K. Igarashi, D. Fernando, and K. Nonami, "Autonomous flight control of unmanned small hobby-class helicopter Report 1: Hardware development and verification experiments of autonomous flight control system," J. of Robotics and Mechatronics, Vol.15, No.5, pp. 537-545, 2003.

[3] T. A. Dukes, "Maneuvering heavy sling loads near hover Part I: Damping the pendulous motion," J. of the American Helicopter Society, Vol.18, No.2, pp. 2-11, 1973.

[4] T. A. Dukes, "Maneuvering heavy sling loads near hover Part II: Some elementary maneuvers," J. of the American Helicopter Society, Vol.18, No.3, pp. 17-22, 1973.

[5] C. Poll and D. Cromack, "Dynamics of slung bodies using a single-point suspension system," J. of Aircraft, Vol.10, No.2, pp. 80-86, 1973.

[6] L. S. Cicolani, A. Cone, J. N. Theron, D. Robinson, J. Lusardi, M. B. Tischler, A. Rosen, and R. Raz, "Flight test and simulation of a cargo container slung load in forward flight," J. of the American Helicopter Society, Vol.54, No.3, 2009.

[7] C. M. Ivler, M. B. Tischler, and J. D. Powell, "Cable angle feedback control systems to improve handling qualities for helicopters

with slung loads," AIAA Guidance, Navigation, and Control Conference, Portland, Oregon, 2011.

[8] C. M. Ivler, J. D. Powell, M. B. Tischler, J. W. Fletcher, and C. Ott, "Design and flight test of a cable angle/rate feedback flight control system for the RASCAL JUH-60 helicopter," the American Helicopter Society 68th Annual Forum, Fort-Worth, Texas, 2012.

[9] M. Bernard, K. Kondak, and G. Honmel, "Load transportation system based on autonomous small size helicopters," The aeronautical J., Vol.114, No.1153, pp. 191-198, 2010.

[10] F. E. Udwadia and R. E. Kalaba, "Analytical Dynamics: A new approach," Cambridge University Press, 2007.

[11] M. Bisgaard, J. D. Bendtsen, and A. Cour-Harbo, "Modeling of generic slung load system," J. of Guidance, Control, and Dynamics, Vol.32, No.2, pp. 573-585, 2009.

[12] M. Bisgaard, A. Cour-Harbo, and J. D. Bendtsen, "Adaptive control system for autonomous helicopter slung load operations," Control Engineering Practice, Vol.18, No.7, pp. 800-811, 2010.

[13] C. Adams, J. Potter, and W. Singhose, "Input-Shaping and Model-Following Control of a Helicopter Carrying a Suspended Load," J. of Guidance, Control, and Dynamics, Vol.38, No.1, pp. 94-105, 2015.

[14] F. E. Udwadia and P. Phohomsiri, "Active control of structures using time delayed positive feedback proportional control designs," Structural Control and Health Monitoring, Vol.13, No.1, pp. 536-552, 2006.

[15] F. E. Udwadia, H. von Bremen, and P. Phohomsiri, "Time-delayed control design for active control of structures:principles and applications," Structural Control and Health Monitoring, Vol.14, No.1, pp. 27-61, 2007.

[16] A. G. Ulsoy, "Time-Delayed Control of SISO Systems for Improved Stability Margins," J. of Dynamic Systems, Measurement, and Control, Vol.137, Issue 4, 2015.

[17] M. Sonobe, Z. Chen, M. Miwa, and J. Hino, "Cable angle feedback control for helicopter slung load system using delayed feedback," J. of Unmanned System Technology, Vol.1, No.3, pp. 100-105, 2013.

[18] K. Hazawa, J. Shin, D. Fujiwara, K. Igarashi, D. Fernando, and K. Nonami, "Autonomous flight control of unmanned small hobby-class helicopter, Report 2: Modeling based on experimental identification and autonomous flight control experiments," J. of Robotics and Mechatronics, Vol.15 No.5, pp. 546-555, 2003.

[19] B. Mettler, M. B. Tischler, and T. Kanade, "System identification modeling of a small-scale unmanned rotorcraft for flight control design," J. of the American helicopter society, Vol.47, No.1, pp. 50-63, 2002.

[20] M. B. Tischler and R. M. Remble, "Aircraft and rotorcraft system identification: Engineering methods with flight test examples," AIAA education series, 2006.

Name:
Motomichi Sonobe

Affiliation:
Lecturer, Schools of Systems Engineering, Kochi University of Technology

Address:
Tosayamada-cho, Kami-shi, Kochi 782-8502, Japan

Brief Biographical History:
2007-2009 Assistant Professor, Yuge National College of Technology
2009-2016 Assistant Professor, Tokushima University
2016- Lecturer, Kochi University of Technology

Main Works:
• "Cable angle feedback control for helicopter slung load system using delayed feedback," J. of Unmanned System Technology, Vol.1, No.3, pp. 100-105, 2013.

Membership in Academic Societies:
• The Japan Society of Mechanical Engineers (JSME)
• The Society of Instrument and Control Engineers (SICE)

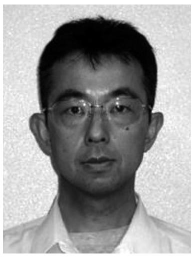

Name:
Masafumi Miwa

Affiliation:
Associate Professor, Institute of Technology and Science, Tokushima University

Address:
2-1 Minami-Josanjima, Tokushima-shi, Tokushima 770-8506, Japan

Brief Biographical History:
1996- Research Assistant, Wakayama University
2007- Assistant Professor, The University of Tokushima
2014- Associate Professor, Tokushima University

Main Works:
• "Ducted Fan Flying Object with Normal and Reverse Ducted Fan Units," Int. J. Robotics and Mechatronics, Vol.1, No.1, pp. 8-15, 2014.

Membership in Academic Societies:
• The Japan Society of Mechanical Engineers (JSME)
• The Robotics Society of Japan (RSJ)
• The Japan Society for Aeronautical and Space Science (JSASS)

Name:
Junichi Hino

Affiliation:
Professor, Institute of Technology and Science, Tokushima University

Address:
2-1 Minami-Josanjima, Tokushima-shi, Tokushima 770-8506, Japan

Brief Biographical History:
1984-1994 Research Assistant, The University of Tokushima
1994-2007 Associate Professor, The University of Tokushima
2007- Professor, The University of Tokushima

Main Works:
• "Identification of Modal Parameters by Frequency Domain Subspace Method (Consideration of Residual Terms and Estimation of Model Order)," Trans. of the Japan Society of Mechanical Engineers, Series C, Vol.79, No.804, pp. 2792-2803, 2013 (in Japanese).

Membership in Academic Societies:
• The Japan Society of Mechanical Engineers (JSME)
• The Society of Instrument and Control Engineers (SICE)
• Japan Society for Design Engineering (JSDE)